Available online at www.sciencedirect.com
SCIENCE DIRECT®
Communications in Nonlinear Science and Numerical Simulation 11 (2006) 13–43
Communications in Nonlinear Science and Numerical Simulation
www.elsevier.com/locate/cnsns

Interaction between flexible shells (plates) and a moving lumped body

V.A. Krysko [a], J. Awrejcewicz [b,*], A.N. Kutsemako [a], K. Broughan [c]

[a] *Department of Mathematics, Saratov State University, 41005 Saratov, Russia*
[b] *Department of Automatics and Biomechanics, Technical University of Lodz, Stefanowskiego 1/15, Lodz, Poland*
[c] *Department of Mathematics, University of Waikato, Private Bag 3105, Hamilton, New Zeland*

Received 6 May 2004; received in revised form 16 June 2004; accepted 18 June 2004
Available online 30 July 2004

Abstract

In this work the problem of interaction between flexible construction and a moving lumped body is reduced to that of essentially simpler ones, i.e. that of vibrations subject to moving force P_0 and that of displacement in the domain of the moving masses under the action of the mentioned force. Advantages of the proposed method are illustrated and discussed.

PACS: 02.30.Hq; 02.30.Jr; 03.40−t; 03.20+i
Keywords: Plates; Shells; Lumped body; Interaction; Constraint; Vibration

1. Introduction

In general, the problem of interaction between moving objects and engineering constructions belongs to important tasks of engineering dynamics. The term ''moving load'' is frequently used in technology nowadays. Movable objects can be either rigid or deformable bodies, fluids, impacting waves, heat or electromagnetic field sources, etc. However, in this contribution, a ''moving

* Corresponding author. Tel.: +48 42 6312378; fax: +48 42 6312225.
E-mail address: awrejcew@p.lodz.pl (J. Awrejcewicz).

1007-5704/$ - see front matter
doi:10.1016/j.cnsns.2004.06.006

load'' or a ''moving body'' is meant to be a load acting either on a plate or a shell created through a weight or an inertial force, or/and moving medium (or bodies).

Dynamical problems of plates and circled cylindrical shells subject to an action of moving objects already have a long history in mechanics. It is mainly motivated by an enormous application of cylindrical shells in the rocket and aircraft industry, as well as the industry of shipbuilding.

Without any doubt, a study of interaction between a landing (starting) aeroplane and an air strip plays a key role in estimating the quality of the plane and the passengers' safety.

Furthermore, in many cases interaction between ship elements and waves is modelled through interaction of a thin-walled structure with a fast moving lumped body.

Another important field where dynamical behaviour of constructions influenced by movable bodies involved has recently been revealed due to the use of nuclear plants. In view of the safety requirements imposed on exploitation of nuclear power plants, designing of construction in housing nuclear reactors must obey high standard norms. It is obvious that among other things, the probability of destruction of such objects is expected to be extremely low, and consequently, the nuclear plants situated, for instance, in the vicinity of airports must be studied with respect to the aeroplane impact. In fact, an isolated construction can be often modelled either as a plate or a shell, while an aeroplane is usually modelled as a system of coupled lumped oscillators.

It is characteristic for the modelling of interaction between a construction and moving bodies that the impact on the construction is expressed by the weight and iterational forces of the objects moving on the studied construction. This crucial feature of the applied approach constitutes also the essential difficulty in the mathematical analysis of the problem.

2. Vibration of construction and moving lumped body (one-sided constraint case)

A mass moving with constant velocity along a surface is subject to the load $P_D(t)$ action, which is nowhere 0 in spite of the contact point between the interacting bodies, and

$$P_D(t) = P - M\frac{\mathrm{d}^2 z_{D,M}}{\mathrm{d}t^2}. \tag{1}$$

In the above, $z_{D,M}$ denotes dynamical transversal mass (lumped body) displacement as well as simultaneous vibrations of the mass and the associated surface; P is the normal component of the weighting force of the body with mass M.

With the origin of the relative coordinate system fixed on the neutral surface of the associated vibrating construction at the point under the body, the introduced coordinate axes are directed along a tangent and a normal to the neutral surface.

Assuming that the mass moves being in contact with the associated surface, the studied motion can be treated as a complex one, i.e. consisting of both the associated surface motion and the relative motion with velocity measured with respect to the surface. In this case one may derive both the mass acceleration in the vertical direction and the vertical component of the mass trajectory using partial derivatives of the dynamical deflection of the associated surface, i.e.:

$$\frac{\mathrm{d}^2 z_{D,M}(x,t)}{\mathrm{d}t^2} = \frac{\mathrm{d}^2 z_D(x,t)}{\mathrm{d}t^2} = \frac{\partial^2 z_D}{\partial t^2} + 2v\frac{\partial^2 z_D}{\partial x\,\partial t} + v^2\frac{\partial^2 z_D}{\partial x^2}.$$

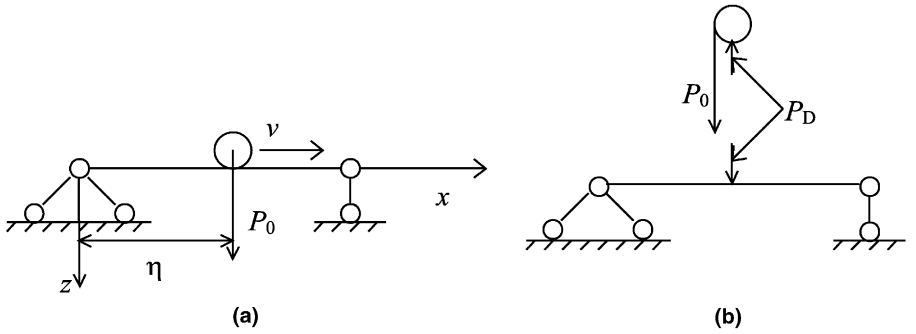

Fig. 1. Scheme of the investigated system: moving lumped body and the associated surface treated as one (a) or two separated (b) systems.

Transversal acceleration $\frac{d^2 z_{D,M}(x,t)}{dt^2}$ of the point mass measured in the fundamental coordinates x, y (Fig. 1) consists of the transitional acceleration $\partial^2 z_D/\partial t^2$ (where z_D denotes deflection of the associated surface under the mass), the Coriolis acceleration $2v\partial^2 z_D/(\partial x\,\partial t)$ generated by a rotation of the relative system during vibrations of the elastic surface, and the relative (oriented into the centre) acceleration $v^2\partial^2 z_D/\partial x^2$.

Since during a contact the body movement $z_D(x,t)|_{x=vt} = z_{D,M}(t)$, and since for each time instant the mass and the point of the associated surface (situated under the mass) vibrate transversally as one body (Fig. 1a), the mass pressure in relation (1) can be expressed through the function of transversal deflections of the associated surface, i.e.

$$P_D(t) = P - M\left(\frac{\partial^2 z_D}{\partial t^2} + 2v\frac{\partial^2 z_D}{\partial x\,\partial t} + v^2\frac{\partial^2 z_D}{\partial x^2}\right)\Bigg|_{x=vt}. \tag{2}$$

Note that the beam vibrations subject to the action of the moving force (2) can be reduced through the Englis–Bolotin method to the system of differential equations yielding the values of transversal beam vibrations z_D [2].

On the other hand, the equation of beam vibrations with the load (2) can be reduced to either integral–differential, or integral, or algebraic equations [3]. During the mentioned reduction process the occurrence of two-sided constraints applied to the mass moving along a smooth surface guarantees the continuous contact between two objects.

However, experimental investigations indicate a possibility of the contact lack between the body and the associated beam (surface). In view of the latter observation our mechanical system consisting of the mass and the associated elastic surface is divided into two components (see Fig. 1b). In what follows two different problems will be studied.

First, the problem of transversal mass displacement subject to the forces of external and dynamical reaction P_D is examined. The second problem analysed is that transversal vibrations of the interacting construction subject to an action of unknown moving force P_D. The values of the pressure generated by the moving lumped body and dynamical reaction are equal, since they play the roles of action and reaction.

Comparison of the mass displacement in the direction normal to the surface and the transversal displacement of the construction under the force action allows derivation of the condition of intersection of the moving mass trajectory and the deformed surface of the associated construction.

When the mentioned interaction is realized, i.e. the mass lies on the associated surface, one gets a positive value of force P_D applying the conditions of equal displacements (force directions associated with the mass moving on the surface is shown in Fig. 1).

Under one-sided constraint, the mass loses its contact with the surface for $P_D \leqslant 0$ and exhibits its own independent motion. In this case $P_D = 0$ is taken for further consideration. Then, an impact occurs when P_D changes its sign.

It is worth noticing that the mass moving along the deformable surface can be treated as a mechanical system with non-stationary holonomic constraints of the form

$$f(x, y, z, t) = 0, \tag{3}$$

and hence it has two degrees of freedom. Virtual mass displacements (allowed by the constraint) will be denoted by $(\delta x, \delta y, \delta z)$, whereas the dynamical constraint reaction is denoted by $P_D(P_{Dx}, P_{Dy}, P_{Dz})$.

Note that relation (3) holds also for virtual displacements, i.e.

$$f(x + \delta x, y + \delta y, z + \mathrm{d}z, t) = 0. \tag{4}$$

Since the constraint is holonomic, formulas (3) and (4) yield

$$\delta f = \frac{\partial f}{\partial x}\delta x + \frac{\partial f}{\partial y}\delta y + \frac{\partial f}{\partial z}\delta z = 0. \tag{5}$$

Note that time has not been variated while deriving (5) because the virtual displacements are not matched with the mass motion. Since in the mechanical system the virtual work of reaction is equal to 0, one gets

$$P_{Dx}\delta x + P_{Dy}\delta y + P_{Dz}\delta z = 0. \tag{6}$$

Both relations (6) and (5) are linear. Furthermore, the linear form of (6) is a linear combination of (5), and therefore

$$P_{Dx} = \lambda\frac{\partial f}{\partial x}, \quad P_{Dy} = \lambda\frac{\partial f}{\partial y}, \quad P_{Dz} = \lambda\frac{\partial f}{\partial z}, \tag{7}$$

where λ is the positive Lagrange multiplier (it characterizes normal reaction force).

The d'Alembert principle yields

$$(X - M\ddot{x})\delta x + (Y - M\ddot{y})\delta y + (Z - M\ddot{z})\delta z = 0, \tag{8}$$

where X, Y, Z are components of active forces acting on mass M.

Multiplying δf by λ in (5) and extracting $\lambda\,\delta f$ from (8), one obtains

$$\left(X - M\ddot{x} - \lambda\frac{\partial f}{\partial x}\right)\delta x + \left(Y - M\ddot{y} - \lambda\frac{\partial f}{\partial y}\right)\delta y + \left(Z - M\ddot{z} - \lambda\frac{\partial f}{\partial z}\right)\delta z = 0. \tag{9}$$

Since from the three possible displacements only two are independent, λ can be taken arbitrarily. Let us take λ satisfying the relation

$$X - M\ddot{x} - \lambda \frac{\partial f}{\partial x} = 0, \tag{10}$$

and assume that δy and δz are arbitrary and independent quantities.

Formula (9) yields

$$Y - M\ddot{y} - \lambda \frac{\partial f}{\partial y} = 0,$$

and

$$Z - M\ddot{z} - \lambda \frac{\partial f}{\partial z} = 0. \tag{11}$$

Two latter dependences and conditions (10) create the first order Lagrange equations.

In a general case, when the mass moves along the deformable surface, Eq. (3) takes the form

$$z(t) - z_i(x, y, t) - z_{i\mathrm{cb}}(x, y, t) - \alpha_{\mathrm{c}}(x, y, t) = 0, \tag{12}$$

where: z is the vertical mass displacement; z_i is the displacement of the surface under the mass; $z_{i\mathrm{cb}}$ stands for the distribution of local surface irregularities of contacting bodies; α_{c} denotes the bodies contact close-up.

Assuming that a rule for the mass motion on the associated surface in plane x, y is given, only Eq. (11) will be further studied.

For small construction deflection and small surface irregularities, the following estimation holds: $P_{Dz} \approx P_D$; $Z = P_0 = Mg$, where g is Earth gravity acceleration.

Owing to relation (7), vertical mass displacement (11) takes the following form

$$P_0 - \frac{P_0}{g} \frac{\mathrm{d}^2 z}{\mathrm{d}t^2} - P_D = 0. \tag{13}$$

Observe that if $z_{DM} = z$, and for $P = P_0$; $M = P_0/g$, Eq. (13) overlaps with (1).

In what follows the analysed problem of dynamical interaction of movable mass on the deformable associated surface is reduced to determination of the unknown dynamical reaction P_D from Eq. (12).

Note that the proposed method improves dynamical model, allows for the contact lack between the mass and surface, and predicts the next contact associated with an impact, but allows also for the introduction of new dynamical factors. Namely, it enables the accounting for local deformations in the contact bodies as well as irregularities of the surface.

On the other hand, Eq. (12) generalizes Timoshenko's equation for the simple impact [1], since the mass approaching the interacting surface may have both vertical and horizontal components.

Furthermore, the case of two-sided constraint can be also derived from Eq. (12). In the latter case, the change of sign of P_D does not yield lack of the contact between the lumped body and the surface.

There is one more advantage of the presented approach. A solution to the problem of dynamical impact of the moving masses on machines and construction elements is essentially simplified. It is reduced to an independent analysis of much simpler problems of construction vibrations driven by movable force P_D, and of displacement of the moving lumped body.

3. Moving load equations

Let us consider a shell with coordinate z directed to the Earth centre, assuming that the body moving in the gravity field possesses the point mass M_T. In what follows both sloping ($v_G \neq 0$) and transversal ($v_B \neq 0$) impacts will be considered.

It is further assumed that the body may move on the shell only after a sloping impact, and its velocity is parallel either to axis x or y. In order to define the mass displacement in directions z, through Eq. (13) one obtains

$$M_T \frac{\mathrm{d}^2 z}{\mathrm{d}t^2} = G_T - P_T, \tag{14}$$

where G_T is the body weight, whereas P_T is the reaction of the interaction between lumped body and the shell.

Let the body move with constant acceleration ω on the shell with initial velocity v_x, parallel to the shell's side with diameter a. Position η of the body is defined through the relation

$$\eta = \frac{\omega t^2}{2} + v_x t. \tag{15}$$

We are going to use the variable η instead of t in Eq. (14).

Making use of the formula

$$\frac{\mathrm{d}z}{\mathrm{d}t} = \frac{\mathrm{d}z}{\mathrm{d}\eta}\frac{\mathrm{d}\eta}{\mathrm{d}t},$$

and owing to (15) one obtains

$$\frac{\mathrm{d}^2 z}{\mathrm{d}t^2} = \frac{\mathrm{d}^2 z}{\mathrm{d}\eta^2}(2\omega\eta + v_x) + \frac{\mathrm{d}z}{\mathrm{d}\eta}\omega, \tag{16}$$

and Eq. (14) expressed in terms of variable η reads

$$\frac{\mathrm{d}^2 z}{\mathrm{d}\eta^2}(2\omega\eta + v_x) + \frac{\mathrm{d}z}{\mathrm{d}\eta}\omega = \frac{G_T - P_T}{M_T}.$$

4. Non-dimensional form of lumped body equations

Since variable t and normal load parameter q occurring in the shell motion equation are transformed to the non-dimensional form (bars) owing to (16), and since reaction P_T of the interaction between the body and the shell is equivalent to shell load, the new non-dimensional parameters are as follows:

$$\eta = a\bar{\eta}, \quad z = (2h)\bar{z}, \quad v_x = \frac{(2h)}{b}\sqrt{\frac{Eg}{\rho}}\bar{v}_x, \quad \omega = \frac{(2h)^2}{ab^2}\frac{Eg}{\rho}\bar{\omega},$$

$$P = \frac{(2h)^4 E}{a^2 b^2}\overline{P}, \quad M_T = \frac{2h\rho}{g}\overline{M}_T, \quad \lambda_1 = \frac{a}{2h}, \quad \lambda_2 = \frac{b}{2h}.$$

Eq. (14) takes the form

$$\frac{\mathrm{d}^2\bar{z}}{\mathrm{d}\bar{t}^2} = \frac{\rho a^2 b^2}{(2h)^3 E} - \frac{\overline{P}_T}{\overline{M}_T}.$$

Let us introduce a new non-dimensional quantity

$$\frac{\rho a^2 b^2}{(2h)^3 E} = \alpha.$$

Since $\overline{M}_T$ is a non-dimensional parameter describing the ratio of the mass body and the mass shell per unit surface, therefore Eq. (14) can be transformed to the following non-dimensional form (index "T" and bars are omitted for simplicity)

$$\frac{\mathrm{d}^2 z}{\mathrm{d}t^2} = \alpha - \frac{P}{M}, \tag{17}$$

where P is reaction force of interaction between load and shell, and M is the ratio of the lumped body and shell masses.

A solution to Eq. (17) in the interval $[t_0, t]$ has the following form

$$z(t) = z_1(t) + z_2(t)(t - t_0) + \int_{t_0}^{t}\left[\alpha - \frac{P}{M}\right](t - \eta)\,\mathrm{d}\eta, \tag{18}$$

where z_1, z_2 are constants defined through the initial conditions.

Continuous function P is approximated by piecewise continuous function $P^{(n)}(t)$ with constant values within small step in time. The introduced approach enables easy computation of integral (18), and hence z and $\mathrm{d}z/\mathrm{d}t$ on each integration step are computed:

$$z(t) = z(t_0) + \left(\alpha - \frac{P}{M}\right)\frac{(t - t_0)^2}{2} + \frac{\mathrm{d}z}{\mathrm{d}t}(t_0)(t - t_0),$$

$$\frac{\mathrm{d}z}{\mathrm{d}t}(t) = \frac{\mathrm{d}z}{\mathrm{d}t}(t_0) + \left(\alpha - \frac{P}{M}\right)(t - t_0). \tag{19}$$

It is obvious that the values of $z(t_0)$ and $\frac{\mathrm{d}z}{\mathrm{d}t}(t_0)$ computed in a previous step serve as initial conditions for the next step.

5. Boundary and initial problem for shell

Consider a rectangular plate cylindrical panel or a spherical shell as the construction interacting with a moving load (see Fig. 2).

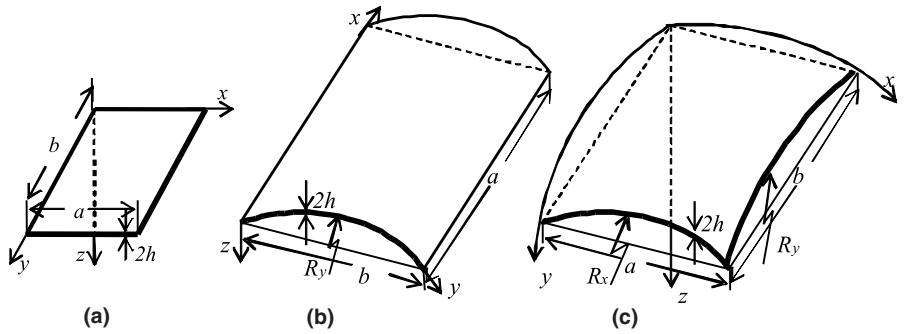

Fig. 2. Rectangular plate (a), cylindrical panel (b), and spherical shell (c) associated with a moving lumped body construction.

Owing to a geometrically non-linear theory and the Kirchhoff–Love kinematical model, the associated of the dynamical hybrid form equations read [4]

$$\frac{\partial^2 w}{\partial t^2}+\varepsilon\frac{\partial w}{\partial t}=\nabla_k^2 F+L(w,F)+q-\frac{1}{12(1-\mu^2)}\left[\frac{1}{\lambda^2}\frac{\partial^4 w}{\partial x^4}+\lambda^2\frac{\partial^4 w}{\partial y^4}+2\frac{\partial^4 w}{\partial x^2\,\partial y^2}\right], \tag{20}$$

$$\frac{1}{\lambda^2}\frac{\partial^4 F}{\partial x^4}+\lambda^2\frac{\partial^4 F}{\partial y^4}+2\frac{\partial^4 F}{\partial x^2\,\partial y^2}=-\nabla_k^2 w-\frac{1}{2}L(w,w), \tag{21}$$

where the operators have the form:

$$\nabla_k^2=k_y\frac{\partial^2}{\partial x^2}+k_x\frac{\partial^2}{\partial y^2},\quad L(w,F)=\frac{\partial^2 w}{\partial x^2}\frac{\partial^2 F}{\partial y^2}+\frac{\partial^2 w}{\partial y^2}\frac{\partial^2 F}{\partial x^2}-2\frac{\partial^2 w}{\partial x\,\partial y}\frac{\partial^2 F}{\partial x\,\partial y}.$$

Note that for the sake of simplicity the bars are again omitted in the mentioned non-dimensional equation, and the relations between the dimensional and non-dimensional parameters are as follows

$$w=2h\bar{w},\quad x=a\bar{x},\quad y=b\bar{y},\quad F=E(2h)^3\overline{F},\quad k_x=\frac{2h}{a^2}\bar{k}_x,\quad k_y=\frac{2h}{b^2}\bar{k}_y,$$

$$q=\frac{E(2h)^4}{a^2b^2}\bar{q},\quad t=\frac{ab}{2h}\sqrt{\frac{\rho_0}{gE_0}}\bar{t},\quad \varepsilon=\frac{2h}{ab}\sqrt{\frac{gE_0}{\rho_0}}\bar{\varepsilon},\quad \lambda=\frac{a}{b}.$$

In order to integrate Eqs. (20) and (21), one has to define boundary and initial conditions.

If the Kirchhoff–Love hypothesis of straight normals is applied, than each contour point should satisfy four boundary conditions. Namely, knowing displacements u,v,w of the curve of contour points it is possible to define the position of the curve after deformation. Note that a normal associated with a contour point may be shifted together with this point and rotated by the value of a

certain angle in the plane normal to the contour curve. To conclude, the normal position after shell deformation is fixed with the help of four quantities.

It is obvious that in a real shell-type construction various support types can be found, which gives a wide spectrum of their mathematical models.

Below, only some of the boundary conditions frequently met in real constructions are reported for $x = 0$; $x = a$ and $y = 0$; $y = b$:

1. Hinged support on flexible ribs non-compressed (non-stretched) in the tangential plane

$$\begin{aligned} &w = M_1 = T_1 = \varepsilon_2 = 0 \quad \text{for } x = 0; a, \\ &w = M_2 = T_2 = \varepsilon_1 = 0 \quad \text{for } y = 0; b. \end{aligned} \tag{22}$$

The above condition can be rewritten in the following form:

$$w = \frac{\partial^2 w}{\partial^2} = F = \frac{\partial^2 F}{\partial y^2} = 0 \quad \text{for } x = 0; a,$$

$$w = \frac{\partial^2 w}{\partial y^2} = F = \frac{\partial^2 F}{\partial x^2} = 0 \quad \text{for } y = 0; b.$$

2. Free edge:

$$w = M_1 = T_1 = S = 0 \quad \text{for } x = 0; a,$$

$$w = M_2 = T_2 = S = 0 \quad \text{for } y = 0; b.$$

3. Movable clamping:

(a)

$$w = 0; \quad \frac{\partial w}{\partial x} = 0; \quad T_1 = \varepsilon_2 = 0 \quad \text{for } x = 0; a,$$

$$w = 0; \quad \frac{\partial w}{\partial y} = 0; \quad T_1 = \varepsilon_2 = 0 \quad \text{for } y = 0; b,$$

(b)

$$w = 0; \quad \frac{\partial w}{\partial x} = 0; \quad T_1 = S = 0 \quad \text{for } x = 0; a,$$

$$w = 0; \quad \frac{\partial w}{\partial y} = 0; \quad T_2 = S = 0 \quad \text{for } y = 0; b.$$

More examples of boundary conditions within the Kirchhoff–Love model are given in monographs [5,6].

Integration of the fundamental equation requires satisfaction of initial conditions associated with deflections and velocities of the mean surface points, i.e.

$$w|_{t=t_0} = \zeta_1(x,y), \qquad \left.\frac{\partial w}{\partial t}\right|_{t=t_0} = \zeta_2(x,y).$$

6. Shell rise

Let us begin with panel rise. Introduce rotations in Fig. 3, where $OD = OF = R$ is the main curvature radius of the mean panel surface; $AF = a$ is the panel dimension in x direction. Then, $H(x_0) = KM = (OB - OC)$ is the sought quantity, which is the panel rise measured at point x_0 in direction x.

From triangles OCF and OBD (see Fig. 3):

$$OC = \sqrt{R^2 - \frac{a^2}{4}}, \qquad OB = \sqrt{R^2 - BD^2} = \sqrt{R^2 - BK^2} = \sqrt{R^2 - \left(\frac{a}{2} - x_0\right)^2}$$

and hence the rise at point x_0 reads

$$H(x_0) = BC = \sqrt{R^2 - \left(\frac{a}{2} - x_0\right)^2} - \sqrt{R^2 - \frac{a^2}{4}}.$$

In order to obtain the rise $H(x_0, y_0)$ at the point with coordinates (x_0, y_0), a coefficient of rise variation for $H(y_0)$ should be introduced, i.e. the ratio of the rise at a point moving along y and the largest rise associated with axis y. It reads

$$\frac{\sqrt{R_y^2 - \left(\frac{b}{2} - y_0\right)^2} - \sqrt{R_y^2 - \frac{b^2}{4}}}{R_y - \sqrt{R_y^2 - \frac{b^2}{4}}}.$$

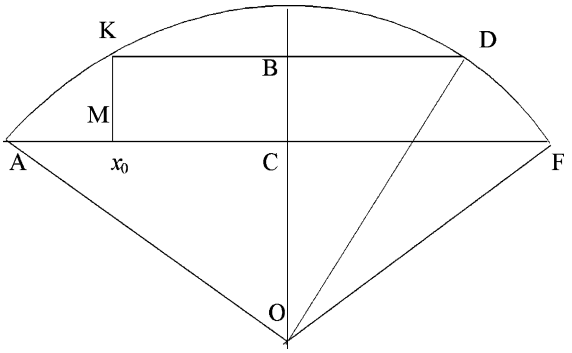

Fig. 3. Panel rise height.

Finally, the shell rise at point (x_0, y_0) follows

$$H(x_0,y_0)=\left[\sqrt{R_x^2-\left(\frac{a}{2}-x_0\right)^2}-\sqrt{R_x^2-\frac{a^2}{4}}\right]\times\frac{\left[\sqrt{R_y^2-\left(\frac{b}{2}-y_0\right)^2}-\sqrt{R_y^2-\frac{b^2}{4}}\right]}{R_y-\sqrt{R_y^2-\frac{b^2}{4}}},$$

and the same holds in the non-dimensional form

$$H(x_0,y_0)=\lambda_1\left[\sqrt{\frac{\lambda_1^2}{k_x^2}-\left(\frac{1}{2}-x_0\right)^2}-\sqrt{\frac{\lambda_1^2}{k_x^2}-\frac{1}{4}}\right]\times\frac{\left[\sqrt{\frac{\lambda_2^2}{k_y^2}-\left(\frac{1}{2}-y_0\right)^2}-\sqrt{\frac{\lambda_2^2}{k_2^2}-\frac{1}{4}}\right]}{\frac{\lambda_2}{k_y}-\sqrt{\frac{\lambda_2^2}{k_y^2}-\frac{1}{4}}},$$

where again bars are omitted for the sake of simplicity.

7. Shell vibrations with two-sided moving lumped body constraints

Let us transform the terms of Eqs. (20) and (21) into their left-hand sides and denote them by Φ_1, Φ_2, respectively. Owing to this transformation, Eqs. (20), (21) read [4]:

$$\Phi_1\left(w,F,\frac{\partial^2 w}{\partial t^2},\frac{\partial w}{\partial t},\frac{\partial^2 w}{\partial x^2},\frac{\partial^2 F}{\partial x^2},q,\ldots\right)=0,\qquad \Phi_2\left(w,F,\frac{\partial^2 w}{\partial x^2},\frac{\partial^2 F}{\partial x^2},\ldots\right)=0. \tag{23}$$

In general, it is impossible to attain an exact solution to these equations with the associated boundary conditions.

Recall that in order to solve the derived equations one may use the Ritz–Timoshenko variational method, the Bubnov–Galerkin approach, the finite difference method, the finite element method, etc.

Owing to the simplification, introduced earlier, of the interaction between the shell and the load moving on it, the Bubnov–Galerkin method can be further used, i.e. the governing equations (20) and (21) will be solved using the Bubnov–Galerkin method with higher approximations. For this purpose, functions w, F, satisfying the boundary conditions, are sought in the form

$$w=\sum_{i,j}A_{ij}(t)\varphi_{ij}(x,y),\quad F=\sum_{i,j}B_{ij}(t)\psi_{ij}(x,y),\qquad i=1,2,\ldots,M_x;\quad j=1,2,\ldots,M_y. \tag{24}$$

Applying the Bubnov–Galerkin procedure to (23), one arrives at

$$\int_0^1\int_0^1\Phi_1\varphi_{vz}(x,y)\,\mathrm{d}x\,\mathrm{d}y=0,\quad \int_0^1\int_0^1\Phi_2\psi_{vz}(x,y)\,\mathrm{d}x\,\mathrm{d}y=0,\qquad v=1,2,\ldots,M_x;\quad z=1,2,\ldots,M_y, \tag{25}$$

and owing to (24) we obtain

$$\sum_{vx}\left[\sum_{ij}\left[\left(\frac{\mathrm{d}^2A_{ij}}{\mathrm{d}t^2}+\varepsilon\frac{\mathrm{d}A_{ij}}{\mathrm{d}t}\right)I_{8,vxij}+A_{ij}I_{1,vzij}.-B_{ij}I_{2,vzij}-qI_{3,vzij}-A_{ij}\sum_{kl}B_{kl}I_{4,vzijkl}\right]\right]=0,$$

$$\sum_{vz}\left[\sum_{ij}\left[A_{ij}I_{7,vzij}+B_{ij}I_{5,vzij}+A_{ij}\sum_{kl}A_{kl}I_{6,vzijkl}\right]\right]=0,\quad v,i,k=1,2,\ldots,M_x;$$

$$z,j,l=1,2,\ldots,M_y. \tag{26}$$

Notice that the summation sign $\sum_{vz}[\bullet]$ standing before each of the equations of (26) means that each of these equations is understood as a system of vz equations, and the associated integrals follow

$$I_{1,vzij}=\int_0^1\int_0^1\frac{E}{12(1-\mu^2)}\left[\frac{1}{\lambda^2}\frac{\partial^2\varphi_{ij}}{\partial x^2}\frac{\partial^2\varphi_{vz}}{\partial x^2}+\lambda^2\frac{\partial^2\varphi_{ij}}{\partial y^2}\frac{\partial^2\varphi_{vz}}{\partial y^2}+2(1-\mu)\frac{\partial^2\varphi_{ij}}{\partial x\,\partial y}\frac{\partial^2\varphi_{vz}}{\partial x\,\partial y}\right.$$

$$\left.+\mu\left(\frac{\partial^2\varphi_{ij}}{\partial x^2}\frac{\partial^2\varphi_{vz}}{\partial y^2}+\frac{\partial^2w}{\partial y^2}\frac{\partial^2\varphi_{vz}}{\partial x^2}\right)\right]\mathrm{d}x\,\mathrm{d}y,$$

$$I_{2,vzij}=\int_0^1\int_0^1-\left(k_y\frac{\partial^2\psi_{ij}}{\partial x^2}+k_x\frac{\partial^2\psi_{ij}}{\partial y^2}\right)\varphi_{vz}\,\mathrm{d}x\,\mathrm{d}y,$$

$$I_{3,vzij}=\int_0^1\int_0^1\varphi_{vz}\,\mathrm{d}x\,\mathrm{d}y,$$

$$I_{4,vzijkl}=\int_0^1\int_0^1L(\varphi_{ij},\psi_{kl})\varphi_{vz}\,\mathrm{d}x\,\mathrm{d}y,$$

$$I_{5,vzij}=\int_0^1\int_0^1a_1\left[\left(\lambda^2\frac{\partial^2\psi_{ij}}{\partial y^2}-\mu\frac{\partial^2\psi_{ij}}{\partial x^2}\right)\frac{\partial^2\psi_{vz}}{\partial y^2}+\left(\frac{1}{\lambda^2}\frac{\partial^2\psi_{ij}}{\partial x^2}-\mu\frac{\partial^2\psi_{ij}}{\partial y^2}\right)\frac{\partial^2\psi_{vz}}{\partial x^2}\right.$$

$$\left.+2(1+\mu)\frac{\partial^2\psi_{ij}}{\partial x\,\partial y}\frac{\partial^2\psi_{vz}}{\partial x\,\partial y}\right]\mathrm{d}x\,\mathrm{d}y, \tag{27}$$

$$I_{6,vzijkl}=\int_0^1\int_0^1\frac{1}{2}L(\varphi_{ij},\varphi_{kl})\psi_{vz}\,\mathrm{d}x\,\mathrm{d}y,$$

$$I_{7,vzij}=\int_0^1\int_0^1-\left(k_y\frac{\partial^2\varphi_{ij}}{\partial x^2}+k_x\frac{\partial^2\varphi_{ij}}{\partial y^2}\right)\psi_{vz}\,\mathrm{d}x\,\mathrm{d}y,$$

$$I_{8,vzij} = \int_0^1 \int_0^1 \varphi_{ij}\varphi_{vz}\,\mathrm{d}x\,\mathrm{d}y. \tag{28}$$

Integrals (27), perhaps apart from $I_{3,vzij}$, where the transversal load acts only on part of the shell, are computed with respect to the whole mean shell surface.

To sum up, system (26) consists of $M_x * M_y$ non-linear second order differential equations with respect to time, and $M_x * M_y$ algebraic equations which are linear with respect to B_{ij}.

Let us describe the mentioned procedure in more detail. For this purpose φ_{ij}, ψ_{ij} from (24) are presented in the product form of two functions, where each of them depends only on one argument and can be presented as a linear combination of functions satisfying the boundary conditions:

$$\varphi_{ij}(x,y) = \varphi_{1ij}(x)\varphi_{2ij}(y), \qquad \psi_{ij}(x,y) = \psi_{1ij}(x)\psi_{2ij}(y). \tag{29}$$

In order to trace the influence of the load parameters on interaction with the shell, the following boundary conditions are further applied

$$w = 0, \quad \frac{\partial^2 w}{\partial x^2} = 0, \quad F = 0, \quad \frac{\partial^2 F}{\partial x^2} = 0 \quad \text{for } x = 0; 1,$$

$$w = 0, \quad \frac{\partial^2 w}{\partial y^2} = 0, \quad F = 0, \quad \frac{\partial^2 F}{\partial y^2} = 0 \quad \text{for } y = 0; 1.$$

Owing to (27)–(29), one obtains

$$\begin{aligned} &\varphi_{1i}(x) = \psi_{1i}(x) = \sin(i\pi x), \quad i = 1, 2, \ldots, M_x, \\ &\varphi_{2j}(y) = \psi_{2j}(y) = \sin(j\pi y), \quad j = 1, 2, \ldots, M_y. \end{aligned} \tag{30}$$

Putting (30) into (24), one gets

$$w = \sum_{i,j} A_{ij}(t)\sin(i\pi x)\sin(j\pi y), \qquad F = \sum_{i,j} B_{ij}(t)\sin(i\pi x)\sin(j\pi y),$$

where indices i,j may take all values.

After application of the Bubnov–Galerkin procedure, system (25) is recast into the following form

$$\int_0^1 \int_0^1 \Phi_1 \sin(v\pi x)\sin(z\pi y)\,\mathrm{d}x\,\mathrm{d}y = 0,$$
$$\int_0^1 \int_0^1 \Phi_2 \sin(v\pi x)\sin(z\pi y)\,\mathrm{d}x\,\mathrm{d}y = 0, \qquad v = 1, 2, \ldots, M_x, \quad z = 1, 2, \ldots, M_y.$$

The integrals of the Bubnov–Galerkin procedure read

$$I_{1,v} = \int_{x_0-\Delta x}^{x_0+\Delta x} \sin(v\pi x)\,\mathrm{d}x = \frac{2}{v\pi}\sin(v\pi x_0)\sin(v\pi\Delta x), \tag{31}$$

$$I_{2,z} = \int_{y_0-\Delta y}^{y_0+\Delta y} \sin(z\pi y)\,\mathrm{d}y = \frac{2}{z\pi}\sin(z\pi y_0)\sin(z\pi\Delta y), \tag{32}$$

where x_0, y_0 are coordinates of the centre of a rectangular contact surface point, Δx, Δy denote half-width of this part with respect to x and y, respectively, and

$$I_{3,vi} = \int_0^1 \sin(i\pi x)\sin(v\pi x)\,\mathrm{d}x = \begin{cases} \frac{1}{2}, & i = v, \\ 0, & i \neq v, \end{cases}$$

$$I_{4,zj} = \int_0^1 \sin(j\pi y)\sin(z\pi y)\,\mathrm{d}y = \begin{cases} \frac{1}{2}, & j = z, \\ 0, & j \neq z, \end{cases}$$

$$I_{5,vik} = \int_0^1 \sin(i\pi x)\sin(k\pi x)\sin(v\pi x)\,\mathrm{d}x = \begin{cases} \frac{1}{4\pi}\left[-\frac{\cos\alpha_1\pi}{\alpha_1} - \frac{\cos\alpha_2\pi}{\alpha_2} - \frac{\cos\alpha_3\pi}{\alpha_3} + \frac{\cos\alpha_4\pi}{\alpha_4} + \frac{1}{\alpha_1} + \frac{1}{\alpha_2} + \frac{1}{\alpha_3} - \frac{1}{\alpha_4}\right], & \alpha_l \neq 0; \\ \left[\frac{\cos\alpha_l\pi}{\alpha_l} = 0, \frac{1}{\alpha_l} = 0\right], \quad l = 1,2,3; & \alpha_l = 0, \end{cases}$$

where

$$\alpha_1 = i + k - v, \qquad \alpha_2 = k + v - i,$$

$$\alpha_3 = v + i - k, \qquad \alpha_4 = i + k + v.$$

$$I_{6,zjl} = \int_0^1 \sin(j\pi x)\sin(l\pi x)\sin(z\pi x)\,\mathrm{d}y = \begin{cases} \frac{1}{4\pi}\left[-\frac{\cos\beta_1\pi}{\beta_1} - \frac{\cos\beta_2\pi}{\beta_2} - \frac{\cos\beta_3\pi}{\beta_3} + \frac{\cos\beta_4\pi}{\beta_4} + \frac{1}{\beta_1} + \frac{1}{\beta_2} + \frac{1}{\beta_3} - \frac{1}{\beta_4}\right], & \beta_l \neq 0; \\ \left[\frac{\cos\beta_l\pi}{\beta} = 0, \frac{1}{\beta_l} = 0\right], \quad l = 1,2,3; & \beta_l = 0, \end{cases}$$

where

$$\beta_1 = j + l - z, \qquad \beta_2 = l + z - j,$$

$$\beta_3 = z + j - l, \qquad \beta_4 = j + l + z.$$

$$I_{7,vik} = \int_0^1 \cos(i\pi x)\cos(k\pi x)\sin(v\pi x)\,\mathrm{d}x$$
$$= \begin{cases} \frac{1}{4\pi}\left[\frac{\cos\alpha_1\pi}{\alpha_1} - \frac{\cos\alpha_2\pi}{\alpha_2} - \frac{\cos\alpha_3\pi}{\alpha_3} - \frac{\cos\alpha_4\pi}{\alpha_4} - \frac{1}{\alpha_1} + \frac{1}{\alpha_2} + \frac{1}{\alpha_3} + \frac{1}{\alpha_4}\right], & \alpha_l \neq 0; \\ \left[\frac{\cos\alpha_l\pi}{\alpha_l} = 0, \frac{1}{\alpha_l} = 0\right], \quad l = 1,2,3; & \alpha_l = 0, \end{cases}$$

$$I_{8,zjl} = \int_0^1 \cos(j\pi x)\cos(l\pi x)\sin(z\pi x)\,\mathrm{d}y$$
$$= \begin{cases} \frac{1}{4\pi}\left[\frac{\cos\beta_1\pi}{\beta_1} - \frac{\cos\beta_2\pi}{\beta_2} - \frac{\cos\beta_3\pi}{\beta_3} - \frac{\cos\beta_4\pi}{\beta_4} - \frac{1}{\beta_1} + \frac{1}{\beta_2} + \frac{1}{\beta_3} + \frac{1}{\beta_4}\right], & \beta_l \neq 0; \\ \left[\frac{\cos\beta_l\pi}{\beta_l} = 0, \frac{1}{\beta_l} = 0\right], \quad l = 1,2,3; & \beta_l = 0, \end{cases}$$

$$I_{q,vz} = I_{1,v}I_{2,z}, \qquad I_{AB,vz} = (z^2k_x + v^2k_y)\pi^2 I_{3,vi}I_{4,zj},$$

$$I_{tt,vz} = I_{3,vi}I_{4,zj}, \qquad I_{t,vz} = \varepsilon I_{3,vi}I_{4,zj},$$

$$I_{w,vz} = \frac{\pi^4}{12(1-\mu^2)}\left(\frac{v^4}{\lambda^2} + 2v^2z^2 + \lambda^2z^4\right)I_{3,vz}I_{4,vz},$$

$$I_{B,vz} = \left(\frac{v^4}{\lambda^2} + 2v^2z^2 + \lambda^2z^4\right)\pi^4 I_{3,vz}I_{4,vz},$$

$$I_{vzijkl} = \pi^4[(i^2l^2 + j^2k^2)I_{5,vik}I_{6,zjl} - 2ijklI_{7,vik}I_{8,zjl}].$$

Owing to the introduced integrals, system (26) takes the form

$$\sum_{vz}\left\{\ddot{A}_{vz}I_{tt,vz} + \dot{A}_{vz}I_{t,vz} + A_{vz}I_{w,vz} + B_{vz}I_{AB,vz} - I_{q,vz}q - \sum_{ij}A_{ij}\sum_{kl}B_{kl}I_{vzijkl}\right\} = 0, \tag{33}$$

$$\sum_{vz}\left\{B_{ij}I_{B,vz} - A_{vz}I_{AB,vz} + \frac{1}{2}\sum_{ij}A_{ij}\sum_{kl}A_{kl}I_{vzijkl}\right\} = 0. \tag{34}$$

Again $\sum_{vz}[\bullet]$ means that instead of each of the equations of system (33) and (34), the system of vz equations is taken.

The obtained system of differential equations is reduced to the normal form, and then it is solved using the fourth order Runge–Kutta method. Solving the Cauchy problem at each time step, the Gauss method is applied to solve algebraic system (34).

In the case of continuous contact load movement, the pressure occurring at the place of contact between the shell and the lumped body consists of the mass weight and inertial forces generated by transversal mass vibrations together with the shell. Owing to (17), one obtains

$$P = M\left(\alpha - \frac{\mathrm{d}^2 z}{\mathrm{d}t^2}\right). \tag{35}$$

Let the contact space between the shell and the mass be approximated by rectangle $S(x, y)$ with the sides parallel to the shell sides, where

$$x_0 - \Delta x \leqslant x \leqslant x_0 + \Delta x, \qquad y_0 - \Delta y \leqslant y \leqslant y_0 + \Delta y.$$

Then the integrals associated with the application of the Bubnov–Galerkin method are computed through formulas (31) and (32), where x_0, y_0 describe the rectangular centre, and Δx, Δy are the half-widths with respect to x, y, respectively.

The inertial term $M\frac{\mathrm{d}z^2}{\mathrm{d}t^2}$ in formula (35) is added into the inertial shell term, and $P = M\alpha$ is substituted in Eq. (33) for the normal load parameter q. Note that if the mass is concentrated to a point, then one may use the transition $\Delta x \to 0$, $\Delta y \to 0$, which gives

$$I_{q,vx} = I_{1,v} I_{2,z} = \Delta x \Delta y \sin(v\pi x_0) \sin(z\pi y_0),$$

and the product $\Delta x \Delta y$ should be included in the reaction between the mass and the shell.

Recall that in practice the so called dynamical coefficients are often introduced. For rods and plates, a dynamical coefficient is defined by dividing the dynamical "critical" loading by the Euler-type static quantity. Furthermore, in the case of rods and plates, the critical load values estimated experimentally are close to those found theoretically.

However, in the case of thin-walled shells, derivation of a similar criterion does not belong to simple tasks, since a shell buckling is realized through a sudden jump. The latter process is associated with stability loss "in large".

Let us briefly describe some of the dynamical stability loss criterion, proposed by various authors.

Volmir [7] defines the dynamical stability loss when a fast deflection increase corresponds to small load variations. Shiam et al. [8] propose the first maximum of the load-time dependence as the critical one. In Ref. [9] "the Lyapunov stability" criterion is applied, which is associated with the use of the phase plane of the considered system. This criterion is used for stability investigation in a rectangular spherical shell.

All the mentioned criterions are in good numerical agreement, i.e. the critical loads derived with their help are closed to each other. In our further investigations the Volmir criterion is used.

In order to determine the shell stability loss of the shell-mass system, as well as in order receive some values of the critical parameters governing interaction between the shell and the mass moving on it, a series of computation is carried out.

It has been found that the influence of the non-dimensional parameter of mass M on the shell behaviour is similar to that of the normal load. There are values which can be called critical and before critical ones, i.e. the shell exhibits a stability loss. It has been observed that owing to the

increase of the contact area, the change of configuration instants of shells 2, 3 in Fig. 4b corresponds to shell stability loss.

In Fig. 4, deflection variation at the shell centre with parameters $\lambda = 1$; $k_x = k_y = 24$ is reported when the centre of the rectangular contact area $2\Delta x$ and $2\Delta y$ between shell and mass overlaps with the shell centre. The applied approximation $M_x * M_y$ reads: $5*5$–$9*9$. Curves 1, 2, 3 are associated with the following parameters: $\alpha = 500$; $M = 2; 4; 10$.

In Fig. 5, shell deflection in the cross section $y = 0.5$ for the case corresponding to Fig. 4b (curves 1, 2) is shown. Curves 1, 2, 3, 4 correspond to time instants $t = 0.2; 0.4; 0.6; 0.8$, respectively. For all reported curves the time step of 0.2 has been used. For the cases when mass parameters are chosen so that the shell configuration does not change suddenly (jump), its deflection is rather small (Fig. 5a). It essentially grows (Fig. 5b), when the mentioned jumps (changes of shell configuration) occur.

On the other hand, the non-dimensional parameter α, occurring in the mass equation, may essentially influence the shell stability loss.

Fig. 6 illustrates the dependence of critical parameter α vs the contact dimension of both bodies ($\Delta x = \Delta y$). Curves 1, 2, 3 correspond to lumped body mass values $M = 2; 5; 10$, respectively.

Observe that $\Delta x = \Delta y = 0.2$ is the limiting value. For $\Delta x = \Delta y > 0.2$ there is no significant influence of α, whereas for $\Delta x = \Delta y < 0.2$ this influence is important and increases with the increase of

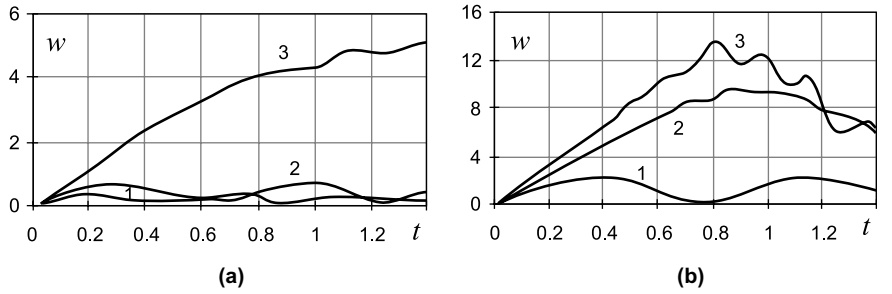

Fig. 4. Variation of the shell centre deflection for different contacting surface areas under the lumped body: $\Delta x = \Delta y = 0.05$ (a), $\Delta x = \Delta y = 0.1$ (b).

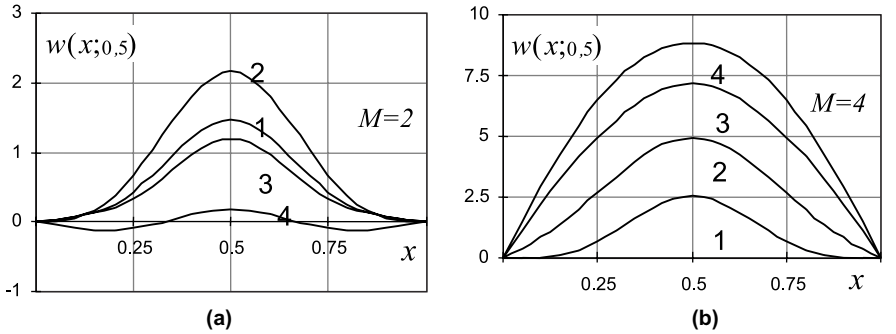

Fig. 5. Diagrams of deflection w in cross section $y = 0.5$ ($M = 2$ (a); $M = 4$ (b)).

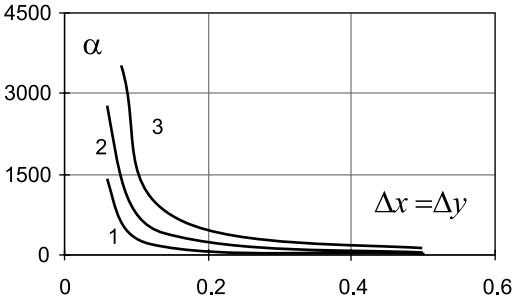

Fig. 6. Critical value of parameter α vs different contact areas under the lumped body.

M. Owing to the mass velocity increase, the largest deflection appears almost suddenly in a zone behind the mass. The same observation holds for the shell, although the shell-mass system is stiffer in comparison with the previously studied one.

8. Shell subjected to transversal rigid body impact

In this section dynamics of rectangular elastic shells during the impact with a rigid body is studied. Again axis z associated with a shell is directed into the Earth centre. It is assumed that while interacting, a lumped body moves on the shell along a line parallel to z.

Therefore, coordinates x_0, y_0 of the first point of the impact remain constant, and only coordinate z_0 is variated. The latter is found using the motion equation the rigid body (17), i.e. it is assumed that during an impact the body may have the vertical velocity component v_B.

In what follows, the process of interaction of the body and shell is considered, with the contact between them, which is either kept for a certain time, i.e.

$$z_0 = w(x_0, y_0) + H(x_0, y_0), \tag{36}$$

or it is violated, i.e.

$$z_0 < w(x_0, y_0) + H(x_0, y_0), \tag{37}$$

where $H(x_0, y_0)$ is the shell rise height at a chosen point.

Conditions (36), (37) governing occurrence of one-sided constraint may interleave many times. However, for a given coordinate system the interaction reaction $P \geqslant 0$.

To solve the defined problem it will be assumed that the shell dynamics is governed by Eqs. (20) and (21).

The Bubnov–Galerkin method of higher approximations is applied to solve the shell dynamics [4].

The system of approximating functions satisfying boundary conditions (22) reads

$$w = \sum_{i,j} A_{ij}(t)\sin(i\pi x)\sin(j\pi y), \quad F = \sum_{i,j} B_{ij}(t)\sin(i\pi x)\sin(j\pi y),$$
$$i = 1, 2, 3, \ldots, M_x; \quad j = 1, 2, 3, \ldots, M_y. \tag{38}$$

The obtained system of the second order differential equations in time is first reduced to the normal form, and then integrated using the 4th order Runge–Kutta method.

The following initial conditions are applied

$$w|_{t=t_0} = 0; \qquad \frac{\partial w}{\partial t}|_{t=t_0} = 0.$$

The lumped body dynamics is solved exactly to yield

$$z|_{t=t_0} = H(x_0, y_0); \qquad \frac{\mathrm{d}z}{\mathrm{d}t}|_{t=t_0} = v_B.$$

Unknown reaction P is estimated at each integration step solving constraint equation (36) and using the Newton method. Since sought quantity P cannot be smaller than 0, $P = 0$ (see (37)) is taken when a contact loss occurs.

With known P all other quantities required for the computations are found, and then taken as initial ones for the next computation step.

Owing to the introduced assumption that the load is either concentrated into a point or is uniformly distributed on a small surface, one has to use a large number of the series terms in (38) and the integration step should be taken satisfactorily small. Satisfaction of the mentioned requirements yields good convergence of the Newton method.

To consider the problem of the dynamical shell stability loss during interaction of the shell with the lumped body, an idea of separation of the dynamics into three stages, as reported in [10], is applied.

In the first stage, the construction vibrates around an initial equilibrium state. The second stage is associated with relatively sudden transition of the shell configuration into a new state. Finally, the third stage deals with non-linear vibrations around the new configuration (equilibrium) position.

The second and the third stage are realized for $P > P_{\mathrm{cr}}$, where P_{cr} is a certain critical value.

In order to investigate influence of the mass and velocity of the impacting body on the mass-shell interaction, the series of computations are carried out. The following values are taken: $k_x = k_y = 24$; $\lambda = 1$; $x_0 = y_0 = 0.5$; $v_B = 0$; $h_t = 0.001$.

Time history of the shell centre deflection for different contact surfaces (a: $\Delta x = \Delta y = 0.05$; $\alpha = 1200$; b: $\Delta x = \Delta y = 0.1$; $\alpha = 400$) is reported in Fig. 7. Curves $1, 2, 3$ correspond to mass $M = 2; 5; 10$, respectively. Time histories of reaction P are shown in Fig. 8 for the same parameters.

From the reported figures one may conclude that the largest shell deflection depends essentially on mass M. One may also introduce a threshold (critical value) of this parameter responsible for stability loss. Increase of the shell-mass contact decreases the values of parameter α required to achieve the same deflections. The shell-mass contact area has a negligible influence on the reaction force.

Observe that the influence of the mass value is important. For the considered parameter set, no lack of mass-shell contact is observed.

If the mass (while impacting) possesses the vertical velocity component $v_B \neq 0$, then its interaction with the shell is qualitatively different. Namely, it may lose its contact with the shell multiple of times.

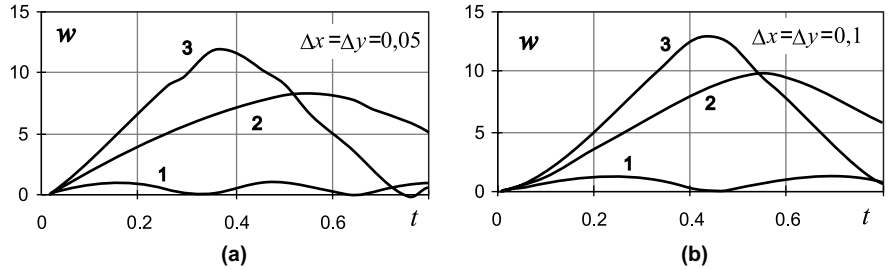

Fig. 7. Variation of shell centre deflection for different contacting surface area under lumped body: $\Delta x = \Delta y = 0.05$ (a), $\Delta x = \Delta y = 0.1$ (b).

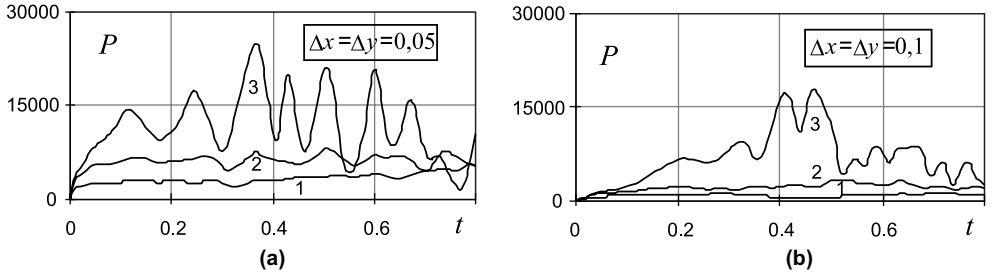

Fig. 8. Variation of shell centre deflection for different contacting surface area under lumped body for $k_x = k_y = 24$ ($\Delta x = \Delta y = 0.05$ (a), $\Delta x = \Delta y = 0.1$ (b)).

For $M = 2; 5; 8; 10$ (curves $1, 2, 3, 4$) the shell centre deflection for $v_B = 80$ is reported in Fig. 9.

For the above mentioned parameters, in all cases considered, lack of contact between the mass and the shell (dotted curve) is exhibited at the beginning of the contact at the time instants at which the shell configuration is changed.

The evolution of reaction P is shown in Fig. 10. Recall that for the lack of the contact zone $P = 0$.

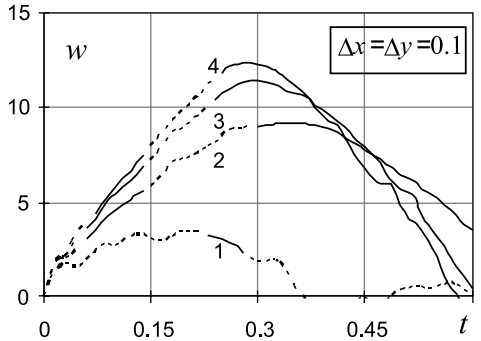

Fig. 9. Shell centre time history ($\Delta x = \Delta y = 0.1$).

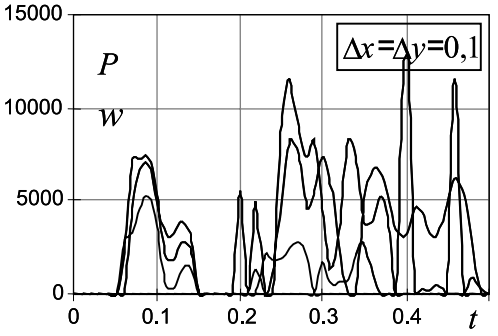

Fig. 10. Shell reaction time history ($\Delta x = \Delta y = 0.1$).

9. Shells with constant velocity moving load

The system of the Bernoulli beam with a mass moving on it belongs to those extensively studied at present. As shown in [1], inertia of the moving mass affects dynamical coefficients in an essential way. For example, the dynamical coefficient for the stress measure is introduced as the ratio of the dynamical stress and static stresses at a beam centre.

Computations show that an increase of mass velocity maxima of dynamical coefficients are shifted along mass displacement, whereas dynamical coefficients associated with deflection and stresses first increase in time, and then (after achieving their maxima) start to decrease.

Our further investigation will focus on the interaction between a load moving with constant velocity along coordinate x and with the mass uniformly distributed on a rectangular area with sides $\Delta x, \Delta y$, and a plate, a panel or a spherical shell serving as the interacting structure.

Note that a moving mass trajectory is identical with the mean curve of an interacting structure, although the input point on the construction can be arbitrary, and the vertical mass velocity component is equal to 0.

Since in this case the mass moves on the shell, it is convenient to use the displacement coordinate along one of the sides of the shell, say x with $\eta = v_x t$, instead of time t (v_x is the mass velocity horizontal component). The mass dynamics is governed by Eq. (17), and it reads

$$v_x^2 \frac{\mathrm{d}^2 z}{\mathrm{d}\eta^2} = \alpha,$$

where now α is equal to $\alpha - \frac{P}{M}$.

In order to solve the second order linear differential equation, the method of variation of constants will be further applied to yield the following solution

$$z(\eta) = z(b) + \frac{\alpha}{2v_x^2}(\eta - b)^2 + \frac{\mathrm{d}z}{\mathrm{d}\eta}(b)(\eta - b), \qquad \frac{\mathrm{d}z}{\mathrm{d}\eta}(\eta) = \frac{\mathrm{d}z}{\mathrm{d}\eta}(b) + \frac{\alpha}{v_x^2}(\eta - b),$$

where $h_1 = (\eta - b)$ is the integration interval (see (19)).

In Fig. 11, the squared shell deflections under the load with mass $M = 5$, $\alpha = 150$ and $v_x = 0.1; 0.5; 2; 5; 8$ (for curves 1–6 respectively) are shown. For small motion velocities (curves 1, 2) the interacting system vibrates with frequency strongly dependent on the mass velocity.

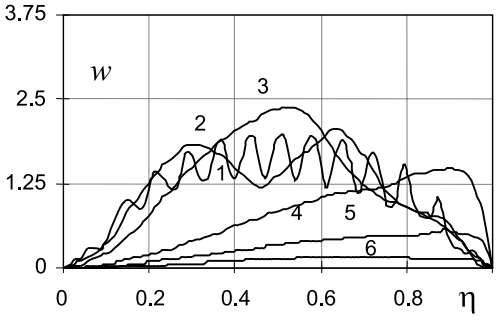

Fig. 11. Dynamical plate deflection caused by a moving load.

With the increase of mass velocity the vibrational process is damped and vanishes (curve 3), and the function that describes the process attains its when the mass goes through the plate centre.

Further increase of the mass velocity shifts the maximal plate deflection to its right side and simultaneously the maximal plate deflection is seriously decreased (curves 4, 5, 6).

In the interaction process between the mass and the plate the lack of contact can be observed. It occurs for small (large) velocities in the case of heavy (light) loading body. Zones of stable and unstable mass-shell contacts in the parameter plane $M - v_x$ are reported in Fig. 12. The zone corresponding to the continuous contact between the two analysed objects is located on the left-hand side.

For parameters $M = 5$, $\alpha = 150$, $v_x = 5$ for the plate ($k_x = k_y = 0$), and the panel ($k_x = 0$, $k_y = 30$) with $\lambda = 2$, the dependencies of deflection under the mass, reaction of self-interaction, forces $T_1 = \partial^2 F/\partial y^2$, $T_2 = \partial^2 F/\partial y^2$, and the moments on the interacting surface are shown in Figs. 13–16.

Although the dependences for the panel correspond to other values, the considered systems are qualitatively similar in character.

In view of the performed computation, the largest plate (or panel) deflection may occur either before or behind the moving mass.

Functions of the largest deflection coordinate of the squared plate $k_x = k_y = 0$ (Fig. 17) and the shell (Fig. 18) with parameters $k_x = k_y = 24$ on a coordinate η describe position of the uniformly moving lumped body.

The straight line 1 corresponds to the moving coordinate, whereas curves 2, 3, 4, 5 correspond to the largest deflection coordinate in given time instants for mass velocities $v_x = 0.5; 2; 5; 10$, respectively.

An analysis of the reported figures yields the following conclusions: for low mass velocities the largest plate deflection occurs first either before or under the mass, and after crossing the plate centre, it moves in a zone behind the mass.

The developed algorithm allows computation of the cases for arbitrary mass point input on the interacting surface, as well as for the mass velocity with horizontal and vertical components.

Deflection variation under the mass for different input points $\eta = 0.25; 0.5; 0.75$ on the plate and panel with parameters $k_x = 0$, $k_y = 30$, $\lambda = 2$ (a: $v_x = 1$, b: $v_x = 5$) are shown in Figs. 19 and 20.

Note that the mass moves along an axial curve of the interacting surface, and its vertical velocity component is equal to 0. The graphs show that if the mass approaches the surface on the right of its centre, then the dynamical deflections are essentially decreased.

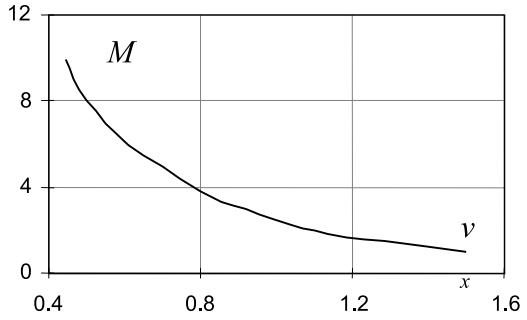

Fig. 12. Stable and unstable contact zones between plate and lumped body.

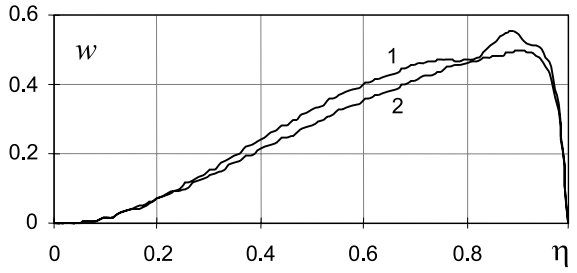

Fig. 13. Dynamical deflection under lumped body (1-plate, 2-panel).

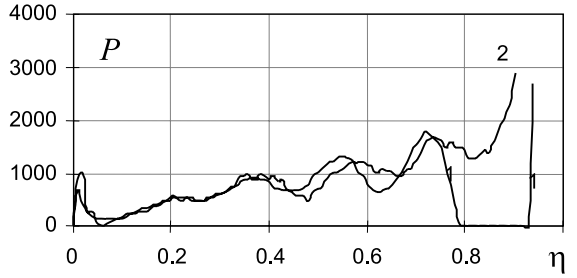

Fig. 14. Reaction (1-plate, 2-panel).

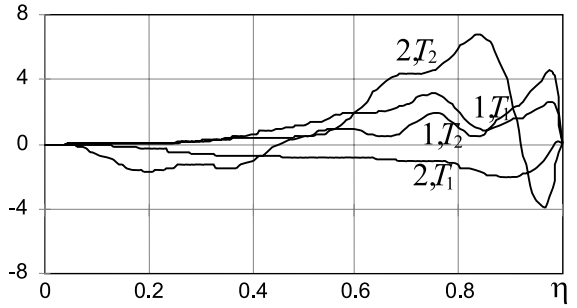

Fig. 15. Forces generated by moving load (1-plate, 2-panel).

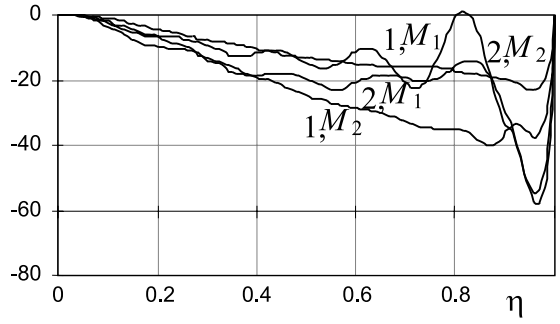

Fig. 16. Moments generated by moving load (1-plate, 2-panel).

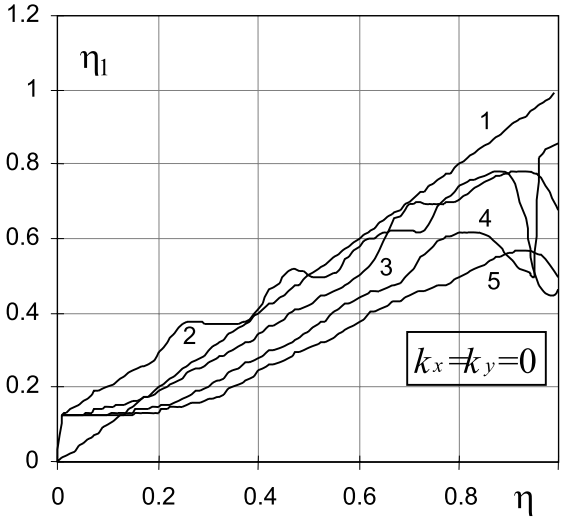

Fig. 17. Largest deflection plate coordinate for a moving load.

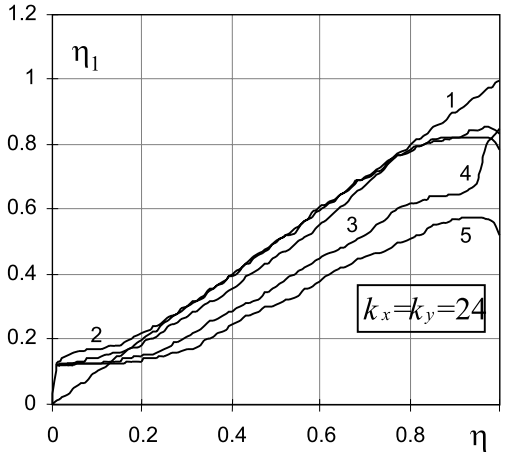

Fig. 18. Largest deflection shell coordinate for a moving load.

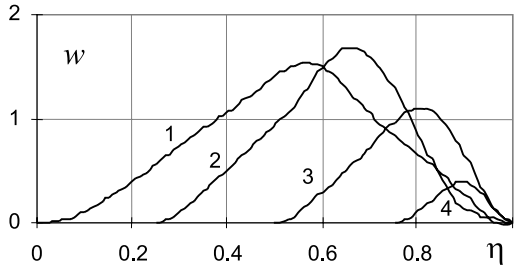

Fig. 19. Plate deflection for various lumped body input points.

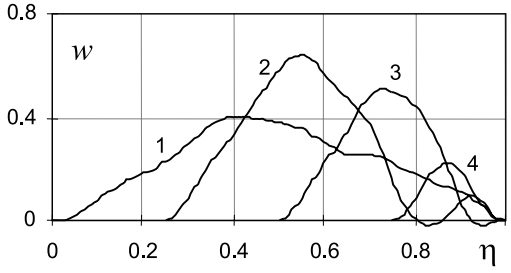

Fig. 20. Panel deflection for various lumped body input points.

In order to compare vibrational regimes of the plate and the shell with a moving mass, appropriate computations have been carried out and the results are reported in the tables below.

In order to receive the values of the investigated parameters included in the tables, which characterize the dynamical processes qualitatively, parameters α and v_x are chosen to be different for the plate and for the shell.

Table 1 displays surface deflection forms w; forces T_1, T_2, and movements M_1, M_2 of the squared plate during transition through the mass along its axial curve ($M = 5$; $\alpha = 150$) with constant velocity $v_x = 5$ for time instants corresponding to $\eta = 0.3; 0.5; 0.7; 0.9$. In Table 2 the same is shown for the shell ($k_x = k_y = 24$; $\lambda = 1$; $M = 5$; $\alpha = 300$, $v_x = 2$). In both cases the mass pressure is uniformly distributed on the area $\Delta x = \Delta y = 0.1$.

Although there are peculiar similarities reported for plates and shells, they differ in stiffness which is decisive for the mass-shell (-plate) interaction.

10. Shell and load moving with constant acceleration

When analyzing mass motion with constant acceleration (positive or negative) instead of time t, it is convenient to use η-coordinate characterizing the load displacement along one of the shell edges (here x).

Namely, let $\eta = \frac{\omega t^2}{2} + v_x t$, where v_x is the mass velocity projection on x for $t = 0$, and ω is the mass acceleration.

Table 1
Plate deflection w, forces T_1, T_2 and moments M_1, M_2 for different η

Plate (k_x=k_y=0)				
	$\eta = 0.3$	$\eta = 0.5$	$\eta = 0.7$	$\eta = 0.9$
w	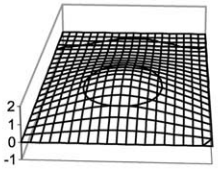	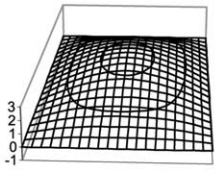	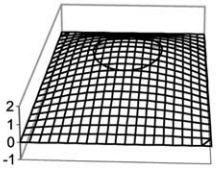	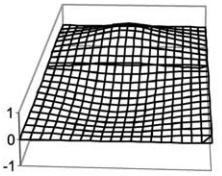
T_1	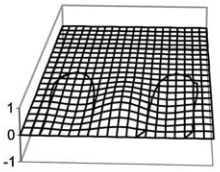	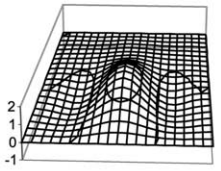	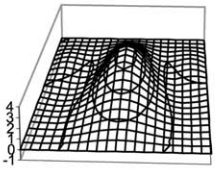	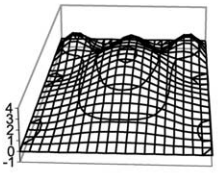
T_2	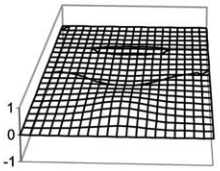	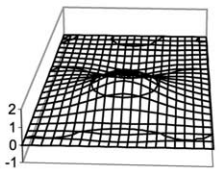	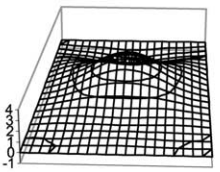	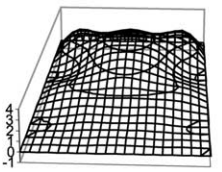
M_1	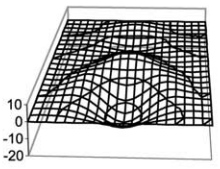	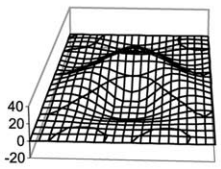	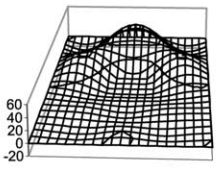	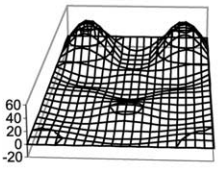
M_2	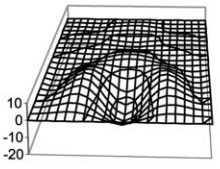	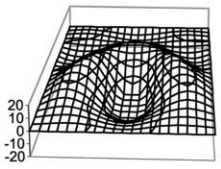	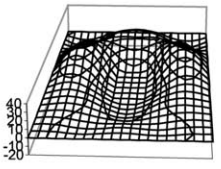	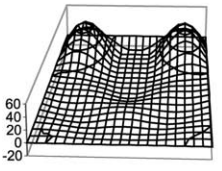

In this case the solution of the mass dynamics governing equation reads

$$z(\eta) = z(b) + \frac{\alpha}{2\omega^2}\left[\sqrt{2\omega\eta + v_x^2} - \sqrt{2\omega b + v_x^2}\right]^2 + \frac{\mathrm{d}z}{\mathrm{d}\eta}(b)\frac{\sqrt{2\omega b + v_x^2}}{\omega}\left[\sqrt{2\omega\eta + v_x^2} - \sqrt{2\omega b + v_x^2}\right],$$

Table 2
Shell deflection w, forces T_1, T_2 and moments M_1, M_2 for different η

Shell (k_x=k_y=24)				
	$\eta = 0.3$	$\eta = 0.5$	$\eta = 0.7$	$\eta = 0.9$
w	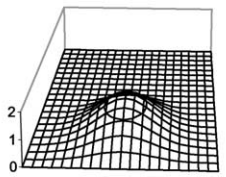	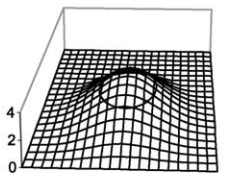	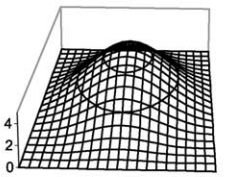	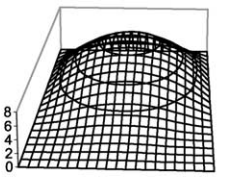
T_1	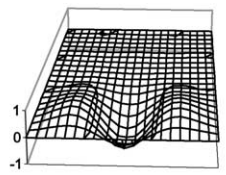	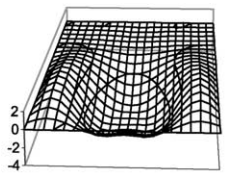	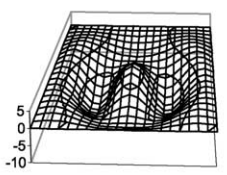	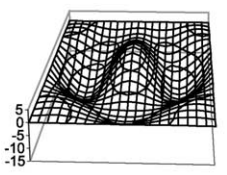
T_2	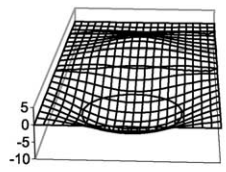	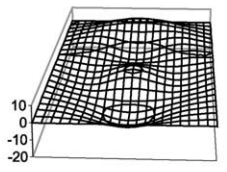	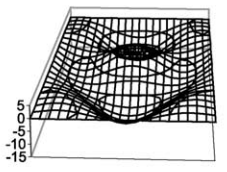	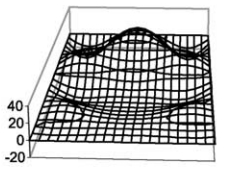
M_1	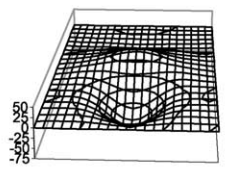	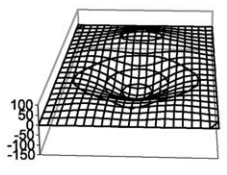	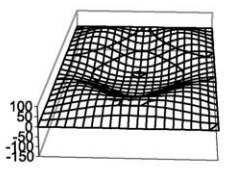	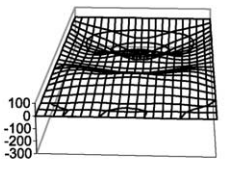
M_2	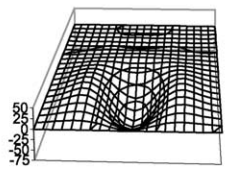	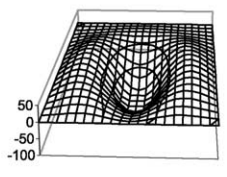	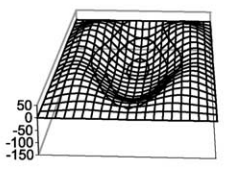	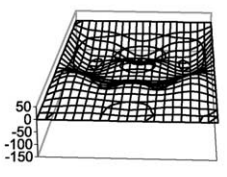

$$\frac{\mathrm{d}z}{\mathrm{d}\eta}(\eta) = \frac{\mathrm{d}z}{\mathrm{d}\eta}(b)\sqrt{\frac{2\omega b + v_x^2}{2\omega\eta + v_x^2}} + \frac{\alpha}{\omega}\left[1 - \sqrt{\frac{2\omega b + v_x^2}{2\omega\eta + v_x^2}}\right].$$

The deflection development under the load for $\alpha = 150$; $M = 5$; $v_x = 1$; $\Delta x = \Delta y = 0.1$ and $\omega = 0; 1; 5; 10; 15; 20; 25$ (curves 1–7, respectively, correspond to mass movement with constant

velocity) is shown for the plate in Fig. 21. The same is done for the shell with the parameters $k_x = k_y = 24$; $\lambda = 1$ (see Fig. 22).

A study of the figures allows the conclusion that for small values of positive acceleration the deflection under the mass (either for plate or shell) does not differ practically from the mass motion with constant velocity (curves 1, 2).

Since acceleration increase causes mass velocity increase, deflections of either plate or shell decrease (curves 2–7). It is expected to occur since the velocity increase does not allow for sudden reaction of the interacting surface.

Furthermore, certain accelerations values may be encountered at which the mass moves with such velocity that the shell does not change its configuration at all (curves 5–7).

11. Shell and load moving with constant negative acceleration

During the load movement with constant negative acceleration ω, its velocity decreases to achieve the zero value for some time instant, i.e. the mass finally stops. Observe that the mass

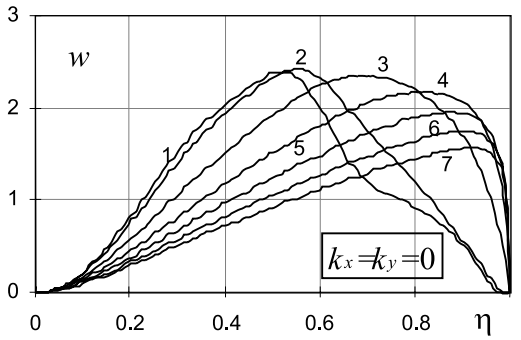

Fig. 21. Plate deflection under the lumped body movement with constant acceleration.

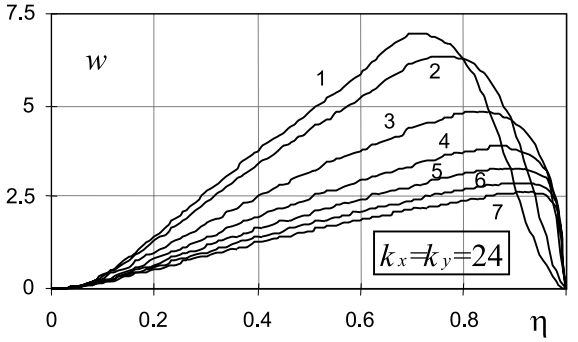

Fig. 22. Shell deflection under the lumped body moving with constant acceleration.

may stop at an arbitrary point of the interacting surface or out of it; the latter case means that when leaving the surface the mass has non-zero velocity.

The analysis to follow will concern the behaviour of both of the interacting mass moving with negative instant acceleration and the construction, under the assumption that the mass stop is given a priori.

Development of deflection under the mass moving on a squared plate, when the mass ($\alpha = 150$; $M = 5$; $\Delta x = \Delta y = 0.1$) begins to move on the plane with the velocity and acceleration such that stops at time instants corresponding to $\eta = 0.5; 0.75; 1; 1.5$ is reported in Figs. 23 and 24.

Note that for $\eta = 1.5$ the mass leaves the construction with non-zero velocity.

The same is done for the panel with parameters $k_x = 0$; $k_y = 30$; $\lambda = 2$ (see Figs. 25 and 26). Curves 1–6 correspond to velocity values $v_x = 1; 2; 3; 4; 5; 6$ of the mass motion beginning on the plate, and for various series of negative acceleration, i.e. $\omega = -1; -4; -9; -16; -25; -36$; $\omega = -0.66; -2.66; -6; -10.66; -16.66; -24$; $\omega = -0.5; -2; -4.5; -8; -12.5; -18$; $\omega = -0.33; -1.33; -3; -5.33; -8.33; -12$ (see Figs. 23a,b, 24a,b, respectively).

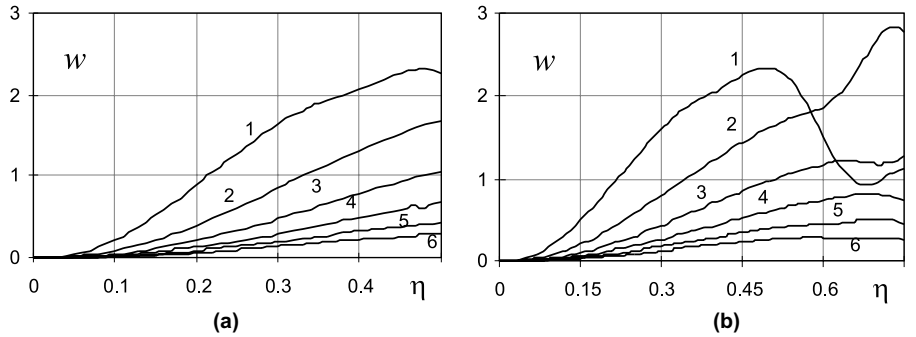

Fig. 23. Plate deflection under the lumped body moving with constant negative acceleration (stop of the lumped body takes place for $\eta = 0.5$ (a) and $\eta = 0.75$ (b)).

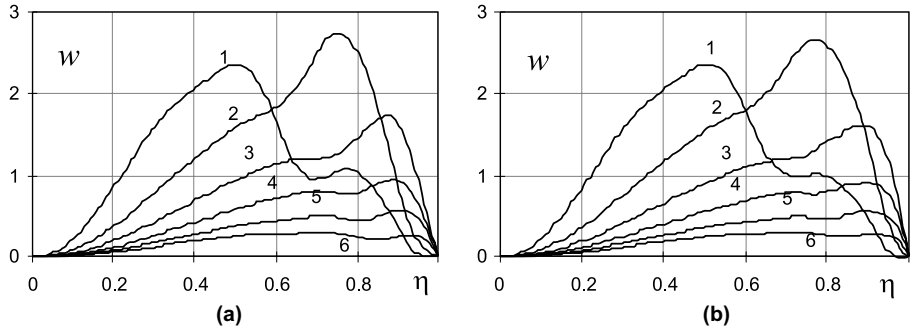

Fig. 24. Plate deflection under the lumped body moving with constant negative acceleration (stop of the lumped body takes place for $\eta = 1$ (a) and $\eta = 1.5$ (b)).

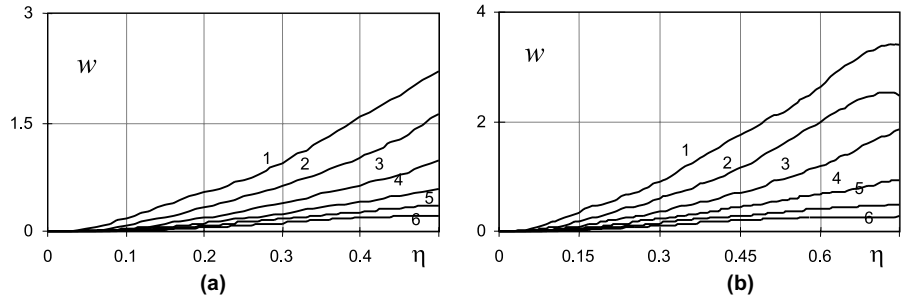

Fig. 25. Panel deflection under the lumped body moving with constant negative acceleration (stop of the lumped body takes place for $\eta = 0.5$ (a) and $\eta = 0.75$ (b)).

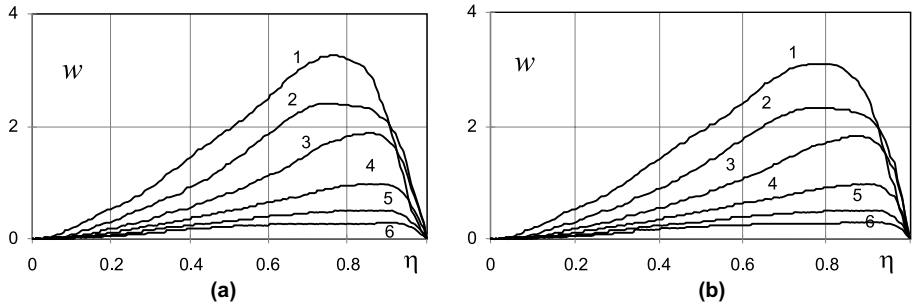

Fig. 26. Panel deflection under the lumped body moving with constant negative acceleration (stop of the lumped body takes place for $\eta = 1$ (a) and $\eta = 1.5$ (b)).

One may conclude from the attached figures that when the mass stops in the centre of the interacted construction, the deflection of the construction increases monotonically until the stop of the mass is achieved.

In the case when the mass stops behind the centre of the construction, an essential role is played by the velocity of the mass at its first contact with the plate. Namely, for small mass velocities, the deflections can be relatively large, but they decrease with the increase of the velocity.

Since for the same parameter selection the panel is stiffer than the plate, therefore the deflection does not achieve the values causing changes in the panel configurations. Such changes may occur for low mass velocities or other choices of parameters (α, M).

12. Concluding remarks

The main results reported in this paper are briefly described below.

A solution to the problem of interaction between moving bodies and machines or construction elements is essentially simplified owing to separation of the two objects. Namely, the problem is reduced to independent solutions of considerably simpler problems of an interacting construction,

i.e. the problem of vibrations subject to moving force P_0 and that of displacement in the domain of the moving masses under the action of the mentioned force.

The proposed method of solution enables (i) improvement of the of dynamics modelling accuracy; (ii) account of the contact lack between interacting objects; (iii) account of successive impacts on interacting surface; (iv) introduction of new dynamical factors useful for engineering application. The fundamental role in the method is played by Eq. (12) governing coupling between two bodies. It may allow for local deformations in an contacting bodies lumped system motion on conical surface roughness with an arbitrary profile, springing support of the moving body, etc.

Since the proposed method of computation of dynamical interaction between a moving body and an associated surface assumes independent integration of the motion equations (in the case of one-sided constraint), the choice of solution methods for the separated equations becomes simplified.

Furthermore, if the motion equations the interacting surface are solved through the Runge–Kutta numerical method, then one may link the corresponding equation of the vertical displacement of the rigid body (14) to allow for the simultaneous interaction of the obtained system equation.

The integration interval of the obtained system is divided into sufficiently large number of equal parts (usually 1000), where the reaction of interaction between objects is assumed to be unchanged within small step duration, which yields practically the exact solution to the problem.

In addition, the proposed partition of the integration interval while seeking dynamical reaction P_0 of the interacting objects from the coupling equation allows achievement of good convergence of the Newton method.

It should be emphasized that the proposed approach to the computation of dynamics of the considered objects does not require any additional restrictions. For example, in the equations governing dynamics of an interacting construction one may include new terms, involving either damping, or non-linearity, or other kinematic models of the interacting surface.

References

[1] Filippov AP. Vibrations of deformable bodies. Moscow: Mashinostroyeniye; 1970 [in Russian].
[2] Bolotin VV. Vibrations of bridges subject to moving load. Mech Mach Designs 1961;4:109–15 [in Russian].
[3] Filippov AP, Kochmaniuk SS. Dynamical interference of moving body loads on rods. Kiev: Naukova Dumka; 1968 [in Russian].
[4] Krysko VA, Kutsemako AN. Stability and vibration of non-homogeneous shells. Saratov: Saratov State University Press; 1999 [in Russian].
[5] Volmir AS. Flexible plates and shells. Moscow: Gostekhizdat; 1956 [in Russian].
[6] Kornishin MS. Non-linear problems of plates and shallow shells and their solutions. Moscow: Nauka; 1964 [in Russian].
[7] Volmir AS. Nonlinear dynamics of plates and shells. Moscow: Nauka; 1972 [in Russian].
[8] Shiam AC, Soong IT, Roth RS. Dynamic buckling of conical shells with imperfections. AIAA J 1974;12(6):262–71.
[9] Krysko VA, Kutsemako AN, Kutsemako DA. Dynamical stability loss of flexible non-linear and elastic shells with sign changeable loads. Saratov: Saratov State University Press; 1995 [in Russian].
[10] Kornishin MS, Serazutdinov MP. Dynamics of shallow shells subject to rigid body transversal impact. In: Statistics and Dynamics of Shells, Proceeding of the Seminar in Kazan, vol. 12, 1979. p. 190–200.